Wave and current effects on floating fish farms

Odd M. Faltinsen[1,2], Yugao Shen[1,2,*]

1. *Department of Marine Technology, Norwegian University of Science and Technology (NTNU) Trondheim, NO-7491, Norway*
2. *Center for Autonomous Marine Operations and Systems (AMOS), NTNU, Trondheim, NO-7491, Norway*

Abstract: The paper is partly a review on hydrodynamic and structural aspects of fish farms. In addition, new numerical results are presented on the stochastic behavior of bending stresses in the floater of a realistic net cage in extreme wave conditions. The behavior of traditional type fish farms with net cages and closed fish farms in waves and current are discussed. Hydroelasticity can play a significant role for net cages and closed membrane-type fish farms. The many meshes in a net cage make CFD and complete structural modeling impracticable. As an example, a hydrodynamic screen model and structural truss elements are instead used to represent the hydrodynamic loading and the structural deformation of the net. In addition, the wake inside the net due to current plays an important role. The described simplified numerical method has been validated by comparing with model tests of mooring loads on a single net cage with two circular elastic floaters and bottom weight ring in waves and current. It is discussed which parts of the complete system play the most important roles in accurately determining the mooring loads. Many realizations of a sea state are needed to obtain reliable estimates of extreme values in a stochastic sea. In reality, many net cages operate in close vicinity, which raises questions about spatial variations of the current and wave environment as well as hydrodynamic interaction between the net cages. Live fish touching the netting can have a non-negligible influence on the mooring loads. It is demonstrated by numerical calculations in waves and current that a well boat at a net cage can have a significant influence on the mooring loads and the bending stresses in the floater. The latter results provide a rational way to obtain operational limits for a well boat at a fish farm.

Sloshing has to be accounted for in describing the behavior of a closed fish farm when important wave frequencies are in the vicinity of natural sloshing frequencies. The structural flexibility has to be considered in determining the natural sloshing frequencies for a membrane-type closed fish farm. Free-surface nonlinearities can matter for sloshing and can, for instance, result in swirling in a certain frequency domain for a closed cage with a vertical symmetry axis.

Keywords: wave, current, aquaculture, net cage, closed fish farm

1 Introduction

The expected increase in world population requires more food. There is a large potential in increasing the marine food production. The total bio production measured in calories is equally divided between land and water (Field et al. 1998). However, only about 2% of the food production used for human consumption comes from water (FAO 2006). Increased aquaculture is therefore expected in the future. There is a trend of

*Corresponding author Email: yugao.shen@ntnu.no

moving marine fish farms to more exposed areas. The fish farms will be subjected to more energetic waves and stronger currents. Furthermore, the dimensions of the fish farms are expected to increase and new designs will appear. The importance of marine technology will consequently increase. Damages and collapses of floating fish farms have led to escape of fish and thereby major economic losses. Damages can be caused by operational failures, breaking of mooring lines, anchor pull out, contacts between chains or ropes with the net or collisions with ships. Escaped farmed salmon may bread with the wild salmon and lead to genetic pollution of the wild fish. Salmon lice is another concern. Multi-trophic aquaculture is used to deal with faeces and feed spills from fish net cages to give nutrients to, for instance, mussels and kelps. Closed fish farms have been installed in order to avoid salmon lice and minimize pollution. Feed availability is a critical factor for sustainable growth of aquaculture. Use of red feed in fish oil has been proposed, which requires design of fishing nets with very small openings.

Sufficient water exchange in a cage matters for the fish health and growth. Important factors are a) available support of oxygen compared to the size and amount of the fish, b) natural current velocity for exercise and well-being of the fish.

We start with discussing wave and current loads on floating fish farms with net cages and go on to study closed fish farms. The influence of a well boat at a floating fish farm with net cage in waves and current is part of the analysis. The approach and departure of a well boat is not handled. Neither is feed barges nor feed hoses, which are important parts of most fish farm systems. Icing and biofouling are also left out. Our studies involve both experimental and numerical studies.

2 Wave and current load effects on floating fish farms with net cages

There exist a variety of floating fish farms with net cages such as circular plastic collar and interconnected hinged steel fish farms. The floater of the circular plastic collar fish farm is made of high-density polyethylene (HDPE) pipes. It is common with two nearly semi-submerged interconnected concentric pipe circles (see Figure 1). An example on dimensions in protected water is 50m diameter and 15m net-cage height. The solidity ratio Sn is an important parameter

of a netting and is for a plane netting the ratio of the area of the shadow projected by wire (twine) meshes on a plane parallel to the screen to the total area contained within the frame of the screen. A typical twine diameter of the net is 3mm. The solidity ratio of the netting may be from 0.15 to 0.32, but biofouling can substantially increase the effective solidity ratio. A bottom weight ring (sinker tube) is often used instead of bottom weights to ensure sufficient volume of the net cage. An idea about wave and current conditions can be found in Table 1.

Figure 1: Floating fish farm with circular plastic collar consisting of two tori that are nearly semi-submerged in calm water, railing, jump net, netting, dead fish removal system, frame of ropes and bottom weights. (Sintef Fisheries and Aquaculture).

Table 1. Norwegian aquaculture site classification for waves and current. H_s = significant wave height; T_p: peak period of the wave spectrum; U_c: current speed (NAS,2009).

Wave	H_s (m)	T_p (s)	Degree of exposure	Current	U_c (m/s)	Degree of exposure
A	0.0-0.5	0.0-2.0	Small	a	0.0-0.3	Small
B	0.5-1.0	1.6-3.2	Moderate	b	0.3-0.5	Moderate
C	1.0-2.0	2.5-5.1	Medium	c	0.5-1.0	Medium
D	2.0-3.0	4.0-6.7	High	d	1.0-1.5	High
E	>3.0	5.3-18.0	Extreme	e	>1.5	Extreme

A consideration is minimum net deformation to ensure sufficient net cage volume. The current deforms the net cage and thereby reduce the net cage volume and affects the current loads. The netting may consequently get in contact with the weight rope or with the chains supporting a bottom weight ring with the possibility of damaging the netting. A not properly designed bottom weight ring may considerably deform in severe weather conditions and damage the net. Large snap loads due to the elastic behavior of the net structure and the relative motion between the floater and the net can occur. Bardestani and Faltinsen (2013) experimentally and numerically predicted the latter fact in nearly 2D flow conditions.

2.1 The floating collar

Kristiansen and Faltinsen (2009) presented model test results in 2D flow conditions of a semi-submerged floater without netting in regular waves and validated a CIP-based finite difference method that solved Navier-Stokes equations for laminar flow with a one-fluid representation of air and water. The CFD calculations illustrated that overtopping of waves and flow separation can matter.

Li et al. (2016, 2017) studied experimentally and theoretically vertical accelerations of a moored floating elastic torus without netting in regular waves of different steepness and periods in deep water. Wavelengths of practical interest are of the order of the torus diameter but long relative to the cross-sectional diameter. An Euler beam model with additional curvature and axial tension effects was applied for vertical and radial torus deformations. 3D flow, hydroelasticity and strong hydrodynamic frequency dependency matter. Strip theory is normally adopted to model the hydrodynamic loads on the floating collar, for example in Huang et al. (2006), Dong et al. (2010), but this may lead to a poor approximation of generalized added mass, damping and wave excitation loads, in particular for vertical loads. The experimental

2

vertical accelerations showed increasing importance of nonlinearities and higher harmonics with increasing wave steepness. Wave overtopping occurred in the steepest waves. A linear frequency-domain potential-flow method gave satisfactory predictions of the first harmonic component of vertical accelerations. This was true by both using state-of-the art boundary element methods as well as the low-frequency linear slender-body theory by Li and Faltinsen (2012). The second harmonic acceleration component can partly be explained by a second-order theory for low wave steepnesses. The experiments showed that the third and fourth harmonic acceleration components matter and cannot be explained by a perturbation method with the wave steepness as a small parameter. Ideally, we need a fully nonlinear 3D CFD method that accounts for hydroelasticity to compare with the experiments.

2.2 The net cage

The fact that the netting may have 10 million meshes limits CFD and complete structural modeling. Kristiansen and Faltinsen (2012) proposed an experimentally based screen type of force model for the viscous hydrodynamic load on nets in ambient current. The model divides the net into a number of flat net panels, or screens. The knots are neglected, and circular twine cross-sections are assumed. The force components on a panel are functions of the solidity ratio, the inflow angle and the Reynolds number. The relevant Reynolds number is that based on the physical twine diameter. Shielding effects by the twines are implicitly accounted for. A uniform turbulent wake is assumed inside the cage based on Løland's (1991) formula for cross-flow past a plane net. The fact that some of the incident flow goes around the net cage is neglected. The latter effect gets increased importance with increasing solidity ratio.

Kristiansen and Faltinsen (2012) used the dynamic truss model by Le Bris and Marichal (1998) and Marichal (2003) to describe the net structure. Number of trusses and their arrangement follow from convergence studies. It is unnecessary to represent the net cage with a fine numerical mesh. The net shape is solved in a time stepping procedure that involves solving a linear system of equations for the unknown tensions at each time step. It means that the problem in current only is solved as an initial value problem instead of iterating to find the steady net configuration. Satisfactory agreement between experimental and numerical prediction of drag and lift on circular bottomless net cages in steady current as function of the solidity ratio of the net and the current velocity is documented. The latter is not true for large current velocities when Morison's equation is applied, which is normally used to estimate the net cage hydrodynamic load (Xu et al. (2013), Shainee et al. (2014)). The reason is associated with large net deformation and shielding effects of twines.

Kristiansen and Faltinsen (2014) investigated the mooring loads on an aquaculture net cage in current and waves by model tests and numerical simulations. Their net model was generalized to combined waves and current and by applying the wake model inside the cage only to the steady flow. The net cage is bottomless, flexible and circular. It is attached to a circular, elastic floater at the top and has 16 sinker weights at the bottom. The system is nearly linearly moored with four crowfeet mooring lines. The simplified mooring system adopted in Kristiansen and Faltinsen (2014) is similar with the bridle lines in the complete mooring system adopted in Shen et al. (2017) (see Figure 2). The mean loads in general dominate over the dynamic part of the loads in combined current and waves, and they significantly increase in long and steep waves, relative to current only. Numerical calculations showed that a rigid floater significantly alters the loads in the mooring lines compared to a realistic, elastic floater. The theoretical model for the wave matters. The mooring loads are rather insensitive to frequency dependent added mass/damping and nonlinear Froude-Kriloff and hydrostatic restoring loads on the floater. Shen et al. (2017) also documented the latter facts.

2.3 Mooring loads of realistic marine fish farms

Many investigations have been performed to investigate the mooring loads of marine fish farms in regular waves and current (Huang et al. (2008), Xu et al. (2013), and in irregular waves (Dong et al. (2010), Xu et al. (2011)). Common to previous works is that the hydrodynamic part of the problem is often over-simplified, for instance the floater was assumed to be rigid and the hydrodynamic forces of the floater were predicted by two-dimensional (2D) hydrodynamic strip theory. The viscous force on the net cage was predicted by Morison's equation, neglecting the shadowing effect of the net and the wake due to current inside the net cage. Also the fish farm including the mooring sytem is simplified compared with a realistic set-up. Shen et al. (2017) presented comparison of numerical calculations with model test results of mooring loads of a marine fish farm in waves and current. The physical model is representative for a single cage commonly used in Norway. It included two concentric floating tubes, an elastic sinker tube, a cylindrical net cage with a conical bottom, mooring system comprising bridle lines, mooring frame lines, mooring buoys, coupling plates, chains connecting the coupling plates to the buoys and the anchor lines attaching the system to the bottom of the basin, see Table 2 and Figure 2. A model test scale of 1:16 was adopted and Froude scaling with geometric similarity except for the net twines was assumed. The reason for Froude scaling in current is the bottom weight system and not gravity waves. We can understand why Froude number matters by considering in calm water a partly submerged vertical net panel that is hinged above the free surface and has a bottom

weight. The equilibrium angle of the panel in current depend on the bottom weight, i.e. acceleration of gravity. In that way the Froude number $U/\sqrt{gL}$ where U is the current velocity and L is a characteristic length becomes a parameter. For the net twines, geometric similarity cannot be applied, as the net twine diameter and net E-module are too small to be realized in model scale if using geometric similarity. So nylon net twines were used in the model tests with correct solidity ratio of the net cage. According to the screen model proposed by Kristiansen and Faltinsen (2012), the solidity ratio and the Reynolds number of the twines are two important parameters to estimate the drag force on the cage. Correct solidity ratio was used in the model test while the Reynolds number of the twine in model-scale (Rn=100-300) is smaller than that in a full-scale cage (Rn=500-1000). Here the cross-section of the net twine is assumed to be circular, which is a reasonable first approximation. In terms of the drag coefficient of the twine, it is larger in model-scale (C_D =1.25-1.35) than that in full-scale (C_D =1.0-1.1). To represent a more realistic full-scale value, we should use as large twine diameter as possible in the model tests to keep the twine Reynolds number as high as possible. Two linear springs were inserted in the front two anchor lines where the forces were measured, as shown in the upper part of Figure 2. The sinker tube was attached directly to the net in the present study, without vertical chains between the floating collar and the sinker tube to avoid chafing between the chain and the net cage.

Shen et al. (2017) used the curved beam equations with axial tension to describe the radial and vertical deformations of the two concentric floating tubes similarly as Li et al. (2016) did for an isolated elastic torus. The deformations were expressed as Fourier series. Hydrodynamic wave-current interaction was neglected. The wave loads and the hydrodynamic loads caused by the radial and vertical deformations, velocities and accelerations were based on linear potential-flow theory. The hydrodynamic radiation loads for different Fourier modes were represented in terms of convolution integrals with retardation functions. The effect of current was described by an empirical viscous drag formulation. The curved beam equations were also applied to the sinker tube. A consequence of the submergence is that the hydrodynamic loads on the sinker tube were approximated by strip theory and the modified Morison's equation with frequency independent added mass coefficients. The net cage (both hydrodynamic and structural) model proposed by Kristiansen and Faltinsen (2012) for a bottomless net cage was adopted for the closed net cage consisting of a cylindrical and a conical part. The mooring system typically comprises ropes and chains, with buoys to support all mooring lines. Ropes and chains are treated in a similar way as the net and are modeled as elastic trusses with correct diameter, weight and stiffness. The hydrodynamic forces on the mooring lines were estimated by the modified Morison's equation based on the cross-flow principle. The buoys are floating circular cylinders. Because the considered wavelengths are long relative to the buoy diameter, a long wave approximation was adopted.

Table 2: Parameters of the floating collar, net cage and sinker tube used in the model tests. Both model-scale (MS) and full-scale values (FS) are given. Since ordinary nylon ropes were used for the net cage in the model tests, the corresponding full-scale E-module (E_{net}) is larger than that used in full-scale cages.

Description	Symbol	Model scale	Full scale	Unit
Floating collar				
Number of tubes	-	2	2	-
Diameter inner tube (center)	D_{f1}	3.125	50	m
Diameter outer tube (center)	D_{f2}	3.2375	51.8	m
Distance between tubes	p	56.25	900	mm
Tube section diameter	d_f	28.125	450	mm
Tube bending stiffness	EI_f	0.72	7.72×10^5	Nm^2
Tube mass	m_f	0.124	32.54	kg/m
Net cage				
Diameter	D_c	3.125	50	m
Depth of vertical net	h_u	0.9375	15	m
Depth of cone net	h_l	0.625	10	m
Net twine diameter	d_w	0.975	3.25	mm
Net mesh-bar length	l_w	7.5	14.3	mm

4

Net E-module	E_{net}	5×10^8	8.2×10^9	N/m²
Center point weight	W_c	0.048	200	kg
Sinker tube				
Tube diameter	D_s	3.2375	51.8	m
Tube section diameter	d_s	17.5	280	mm
Tube depth	h_s	1.0625	17	m
Tube bending stiffness	EI_s	0.195	2.0×10^5	Nm²
Mass per meter in water	w_s	0.095/0.191	25/50	kg/m
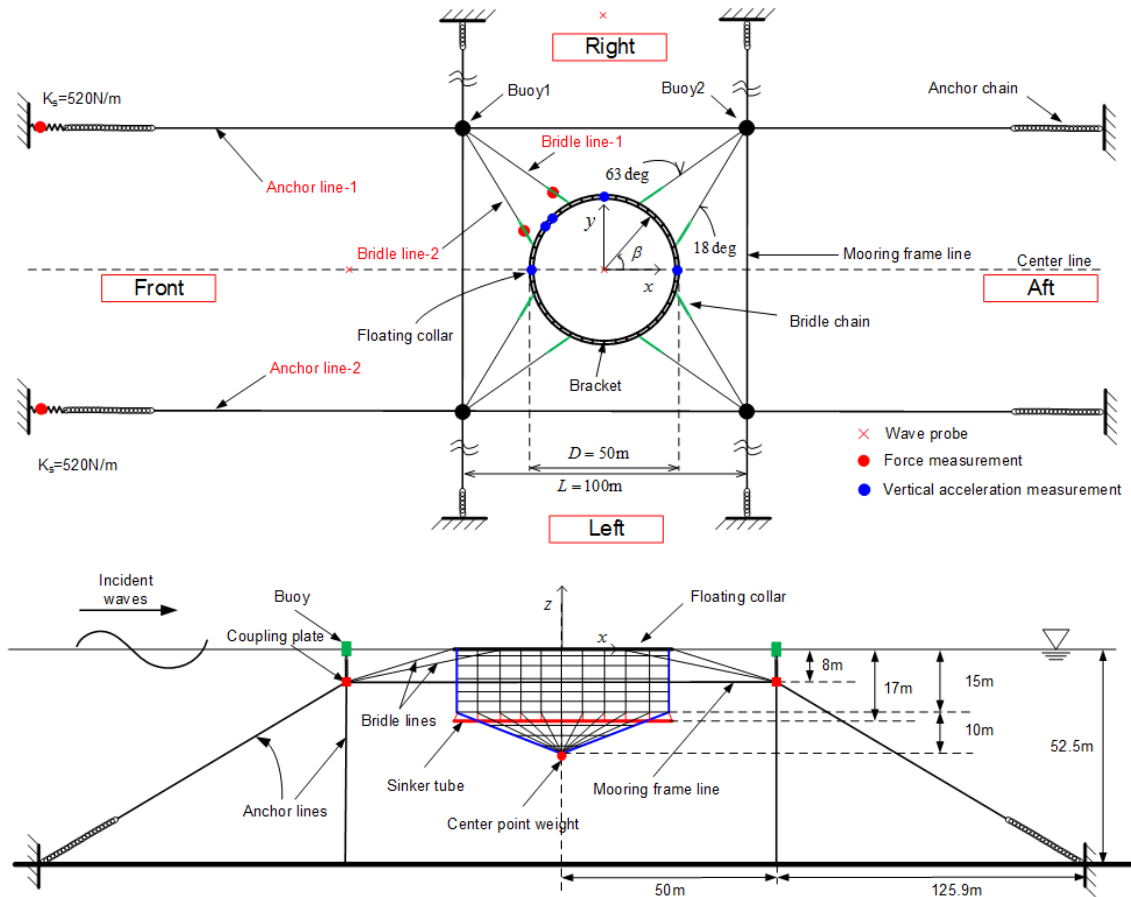
Figure 2. Experimental set-up with full-scale dimensions. Upper: top view. Lower: side view. Two springs were inserted in the front two anchor lines (Shen et al., 2017).

Numerical free-decay tests in surge with calm-water conditions were performed by assuming a rigid floater and full-scale dimensions. The restoring force from the mooring system are due to the axial elasticity of anchor lines, bridle lines and mooring frame lines. If the net was included, the system was overdamped. If the net was disregarded, the estimated natural period was 7.9 seconds, which is very low relative to natural periods in surge of floating offshore structures with a spread mooring system. Second-order wave excited horizontal slow-drift oscillations is of concern for the mooring system in the latter case, while it is not for the considered fish farm.

Numerically calculated drag coefficients for the net cage versus current speed for sinker tube weights 25 kg/m and 50kg/m in full scale conditions are presented in Figure 3. The floater and the sinker tube are assumed
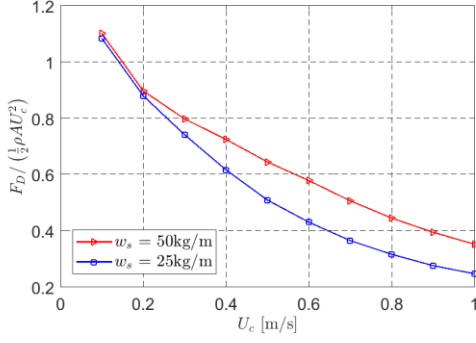
Figure 3. Drag coefficient $C_D = F_D / (0.5\rho U_c^2 A)$ of the net cage as a function of current velocity U_c. Here A is the projected area of the cage without current. Two sinker tube weights $w_s = 50$ kg/m and 25 kg/m are considered.

rigid and the influence of the mooring system is neglected. The projected area of the net cage without current is used to normalize the drag force. The decrease in drag coefficient for small current speeds with increasing current speed is mainly due to decrease in the drag coefficient for a twine with increasing twine Reynolds number. The further decrease of the drag coefficient with increasing current speed are influenced by the sinker tube weight and are mostly due to the reduced projected area.

Experimental and numerical values of the average value of the tensions in the front two anchor lines in current were documented. When the experimental current condition was full scale current velocity 0.5m/s with sinker tube weight 50 kg/m, the relative difference was 14.9%. When the current velocity was 0.7m/s with sinker tube weight 25 kg/m, the relative error was 7.2%.

A numerical sensitivity study of the numerical model in current was performed. The error estimates were obtained by averaging results for current velocities between 0.1m/s and 1m/s. When the drag forces on the two floating tubes are neglected, the anchor force has a 4% reduction, which means that the drag on the floating collar is quite moderate compared with the total drag on the system. So it is not necessary to model the drag force on the floating collar in a very accurate and time-consuming way. Modeling the floating collar and sinker tube as rigid bodies in ambient current has a small effect on the anchor force.

The flow reduction factor in the rear part of the net cage due to the shadowing effect is the most important parameter for the anchor force and the anchor force will increase up to 22% if the shading effect is neglected in ambient current. The weight of the net in water is assumed to be zero in nominal simulations, so the weight of the net equals the buoyancy of the net. The weight of the net in water is slightly larger than zero in reality. Increasing the net weight by 10% in the sensitivity analysis changes the anchor loads by about 7%. Detailed variation of the structural modeling of the net is also considered. Changing the net depth (cylindrical part) and the net solidity ratio by 10% lead to a similar deviation from the nominal value by about 5% to 7%. Increasing the net diameter (conical part) by 10% will lead to larger deviation, about 15%. This is due to a big increase of the net volume, consequently larger drag force on the net. The effect of the net elasticity is also investigated. Ordinary ropes were used in the model tests for the net cage. However, when scaled up using Froude-scaling, the elasticity gives higher stiffness than for the nets used in commercial full-scale cages. A model scale Young's modulus of $E_{net}=6.25\times10^7 N/m^2$ would conform more to a realistic full-scale value, but could be difficult to realize in a model test set-up. So, two different net elasticities were tried in the sensitivity analysis with $E_{net}=6.25\times10^7 N/m^2$ and $E_{net}=5\times10^{10} N/m^2$, which correspond to a realistic full-scale value and to an almost rigid net. Numerical results show that the net elasticity has a small effect on the anchor force as long as it is in a reasonable region such as larger than $10^7 N/m^2$. The point weight that attached to the bottom of the net is also varied and very small deviations are observed.

The pretension forces in the front two anchor lines are asymmetric with respect to the x-axis in the model tests. The x-axis is defined in Figure 2. Asymmetric pretension forces are used in the nominal simulations and negligible difference is observed if mean pretension forces are adopted. The anchor loads do not seem to be sensitive to the stiffness of the springs in the anchor lines, the weight of the anchor chain and the drag forces on the buoys.

Satisfactory agreement of the mooring loads in the front two anchor lines and front two bridle lines in both regular and irregular waves were documented. The experimental regular wave conditions corresponded to full scale wave period T=6s with wave height-to-wave length ratio 1/22 and T=8s with wave height-to-wave length ratio 1/40. The experimental current conditions with the latter wave conditions were zero current velocity and full scale current velocity 0.5m/s. The effect of the sinker tube weight was examined by using sinker tube weights 25kg/m and 50 kg/m. The influence of the sinker tube weight in waves without current is less important than in combined wave and current conditions. The latter fact is related to that the net in current is deformed more the higher the current velocity is and the smaller the sinker tube weight is. A consequence of the deformation in current is change in the projected area and hence the hydrodynamic force on the net cage.

A sensitivity analysis was also performed for the system in regular waves only and in combined regular waves and current. The focus was on the peak (total) values of the mooring loads and the results were for each combined current and wave steepness averaged over wave periods from 3s to 10s. Modeling the sinker tube as a rigid body has a pronounced effect on the anchor load for cases in waves only. A reason is that a rigid sinker tube will change the deformation of the net

in vertical direction, as a rigid sinker tube cannot deform accordingly with the floating collar, which tends to follow the wave profile for longer wavelengths. In combined waves and current cases, the flow reduction factor in the rear part of the net and the diameter of the net cage (conical part) are the two important parameters. The axial stiffness due to axial tensions in the floater has limited effect. In general, the loads on the floating collar are quite moderate compared with forces on the whole system. Sensitivity analysis for the bridle loads are also conducted. Modeling the floating collar as a rigid body has a pronounced effect on the bridle loads. This is because rigid floating collar significantly changes the force distribution along the bridle lines.

Experimental anchor line and bridle line loads in long-crested irregular sea conditions with full-scale current velocity 0.5m/s in the wave propagation direction were compared with the numerical model. The sinker tube weight was 50kg/m. JONSWAP wave spectra with spectrum peakedness 2 were used. The combinations of full scale significant wave height and peak period of the spectrum were (1.0m, 4.0s), (1.5m, 4.5s), (2.0m, 5.0s), (2.5m, 6.0s), (3.0m, 7.0s), (4.0m, 8.0s). Each sea state had 1.5-hour duration in full scale. The mean and maximum values of the mooring loads in the front two anchor lines and front two bridle lines were considered. The pretension forces were subtracted. The mean values of the mooring loads for cases with different significant wave heights and peak wave periods are similar while there is a big difference in the maximum values. Furthermore, the tension in the bridle line-2 is about twice that in the bridle line-1. One of the possible reasons is that the stiffness of the side anchor lines in the model tests is much higher than the corresponding realistic value, so the bridle line-2 is forced to absorb more load. The mean values of the tensions in the bridle line-2 and in the anchor lines are similar, but the maximum tension in the bridle line-2 is much larger. Focus was on the average value of the loads in the front two anchor lines (anchor load) and the load in the bridle line-2 (bridle load). There is general agreement between the numerical and experimental results of the mean, standard deviation and maximum values of the anchor loads and numerical results slightly over-predict the mean values, which is similar with that in current only cases. It should be noted that the random phase seeds used in the experiments to generate the incident irregular waves are different with respect to those used in the simulations. The ratio of the maximum anchor load (minus mean value) to the standard deviation varies from 4.6 to 6.7 according to the experimental data. The latter fact shows that a Rayleigh distribution does not apply and is a consequence of that the velocity-square dependent drag loads on the net cage dominate. There is an analogy to the statistical distribution based on Morison's equation with dominant drag forces (Naess and Moan, 2012).

Numerical simulations with different random phase seeds (in total 20) to generate the incident irregular waves were performed and the comparison of the maximum values of the mooring loads between the numerical and experimental results shows that there is a big variation of the maximum loads in the anchor line and in the bridle line when different random phase seeds are used in the numerical simulations. The maximum anchor loads from numerical predictions vary from 98% to 136% of that from the experiment and the maximum bridle loads change from 74% to 105% of the experimental data. As an engineering practice, at least 10-20 realizations of the same wave spectrum are needed to have a robust estimation of the most probable maximum value which is taken as the mean value of these realizations. In order to have a better comparison of the most probable maximum value between numerical and experimental results, more realizations of the same spectrum in the experiments are needed.

2.4 Bending stresses in the floating collar

The numerical investigations by Shen et al. (2017) have been extended by studying the stress distributions of maximum stress along the floating collar due to horizontal and vertical deformations. The corresponding results are given in Figure 4 for different realizations of a sea state with significant wave height 4m and peak period 8s. The current speed is 0.5m/s. The considered sea state corresponds to a 50-year storm condition for a realistic fish farm site with storm duration 1.5 hours. The figure shows that the maximum stress due to vertical deformations are close to that from horizontal deformations but at different positions and that the maximum stress along the floating collar will not exceed the yield stress for the considered sea state. In the analysis, a linear stress-strain relationship is assumed with an elastic modulus $E_{HDPE} = 1.0$GPa, which is a typical value for the floating collar. The figure also shows that the largest maximum stress occurs at different positions in horizontal and vertical directions. The maximum stresses from different realizations at the radial angle 117 degrees along the floater with zero degrees corresponding to the x- axis defined in Figure 2 are shown in Figure 5. From the figure, we can see that the maximum stress is realization dependent. The Gumbel and Weibull probability distribution functions are commonly used to fit the distribution of the maximum values from different independent realizations. From curve fitting results, shown in Figure 6, we can see that that the Gumbel distribution is more proper to fit the maximum stress in horizontal direction while the Weibull distribution is better for that in vertical direction. We are specifically interested in the Most Probable Maximum Extreme (MPME) value for a given time duration. If the probability distribution for the maximum values is known, then the MPME can be obtained where the probability distribution function

7

reaches maximum. Sometimes, for simplicity, the MPME is taken as the average value of the maximum stresses from different realizations. Our results show that MPME estimated by the two methods are similar.

In reality, many net cages operate in close vicinity, which raises questions about spatial variations of the current and wave environment as well as hydrodynamic interaction between the net cages. For instance, upstream cages modify the incident current to downstream cages.
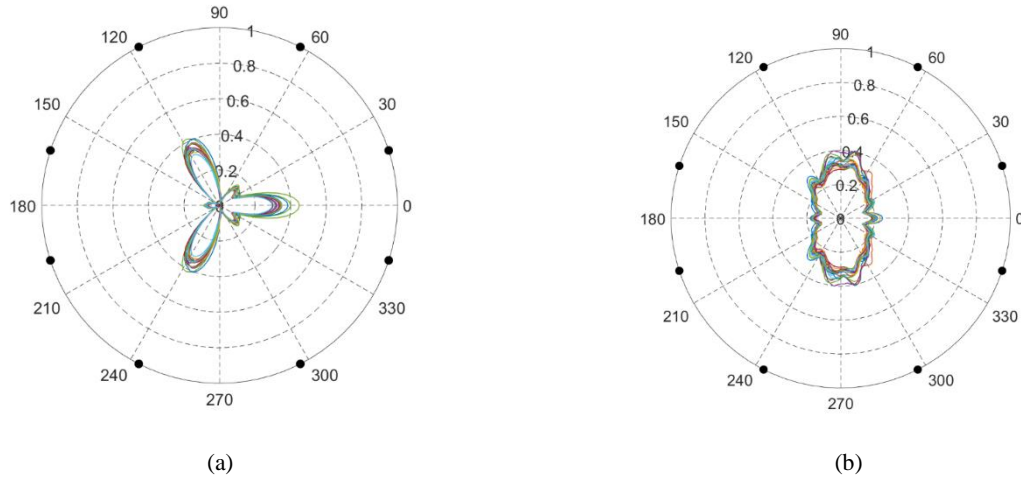

(a)

(b)

Figure 4. Maximum stress distributions along the floating. Current and wave propagation directions are along the x-axis (see Figure 2). Different colors represent different random phase seeds used to generate the incident irregular waves. The stress is made non-dimensional by the yield stress (high-density polyethylene). Solid circle symbols represent the positions where bridle lines are attached. (a) Stress due to horizontal deformations. (b) Stress due to vertical deformations.


(a)

(b)
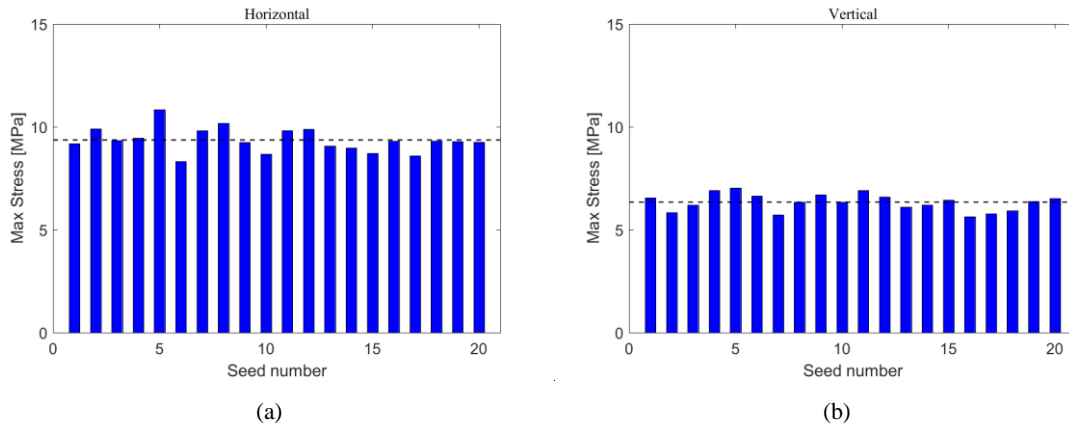
Figure 5. Numerical results for the maximum stress along the floating collar at $\beta = 117^\circ$ (see Figure 2). The environmental conditions are the same as in Figure 4. The numbering along the horizontal axis represents different random phase seeds used to generate the incident irregular waves. Dashed line represents the most probable maximum value obtained as mean among the maximum values from the numerical simulations. (a) Stress due to horizontal deformations. (b) Stress due to vertical deformations.
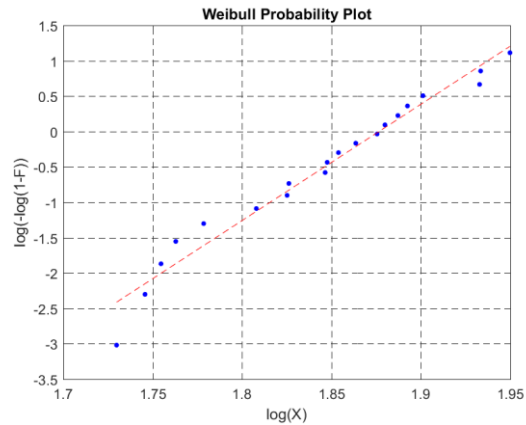
8
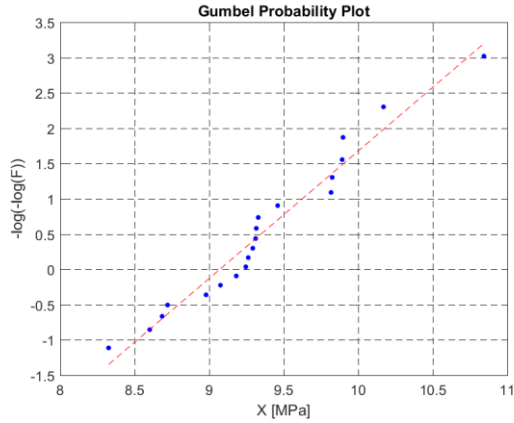
(a) Maximum stress fitted by Gumbel distribution
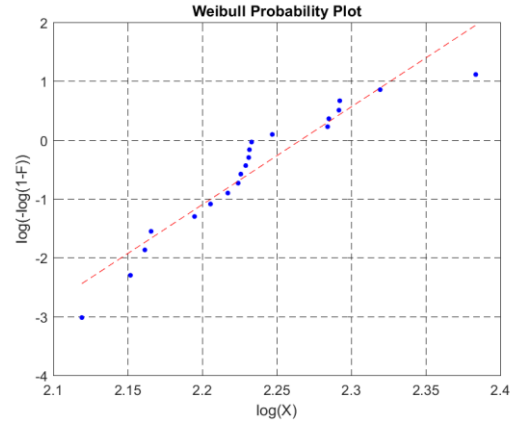
(b) Maximum stress fitted by Weibull distribution
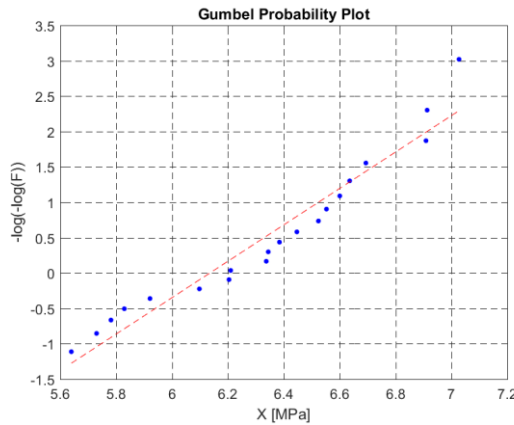
(c) Maximum stress fitted by Gumbel distribution

(d) Maximum stress fitted by Weibull distribution

Figure 6. Probability distribution for the maximum stress due to horizontal (upper row) and vertical (lower row) deformations for the environmental condition described in the caption of Figure 4. X denotes the maximum stress from different realizations and F denotes the cumulative distribution function.

2.5 Influence of a well boat at a fish farm

Shen et al. (2016) investigated numerically a well boat moored at a fish farm in waves and current. Studies as this can provide guidance in establishing operational limits for the loading/offloading phase. The idealized fish farm consisted of a flexible-bottomless net cage with sinker weights at the bottom and attached to an elastic circular floater at the top, and was moored with a realistic mooring line system. Physical connections between the well boat and the floater as well as possible contact forces were also considered. The coupling between the ship and the net cage with mooring caused

a natural period for rigid body motion along the x_E-axis that is much larger than the considered wave periods. The configuration of the well boat and the moored fish farm system when there is no contact between them is illustrated in Figure 7 together with the wave propagation and current directions. The ship draft and length between perpendiculars are 6.7m and 70 m, respectively. The floater diameter, net depth and net solidity ratio are 50m, 25m and 0.26, respectively. Furthermore, the cross-sectional diameter and bending stiffness of the floater are 0.6364m and 2.0×10⁶ Nm²,

respectively. The loading/ offloading condition in waves and current can significantly affect the mooring tension and the structural stresses in the floater. The maximum horizontal bending stresses along the floater in current velocity 0.6m/s and three regular wave conditions with wave height-to-wave length ratio 1/60 are illustrated in Figure 8. For the cases with wave period 6s and 9s, the maximum stresses occur at the positions where the mooring lines at angles 117 degrees and 243 degrees are attached. The latter angle is the radial angle along the floater with zero degrees corresponding to the x_E-axis defined in Figure 7. There is also a local peak value in the contact region between the well boat and the fish farm. The stress at the position with angle 180 degrees grows from T=3 to 6s but decreases at T= 9s, while at angles 117 degrees and 243 degrees, the stress grows with increasing wave period. This is mainly due to the contact and coupling between the boat and the floater. The maximum stress for wave period 9s exceeds the floater yield stress at positions where the bridle lines are attached. The presence of the well boat not only changes the magnitude but also alters

9

the distribution of the stress along the floating collar, as can be seen from the comparison between Figure 4 and Figure.8. In Figure 4, without the well boat, the maximum horizontal stress has three peaks associated with three lobes, at angles 117 degrees, 243 degrees (attachment points of bridle lines) and 0 degree (due to the force from the net cage). In Figure 8, there are also three peaks at angles 117 degrees, 243 degrees and 180 degrees. Two of them (angles 117 degrees and 243 degrees) correspond to the attachment points of bridle lines while the third peak is caused by the loads from the well boat. The influence of the well boat on the vertical deformations of the floating collar is also investigated and small influence is observed.
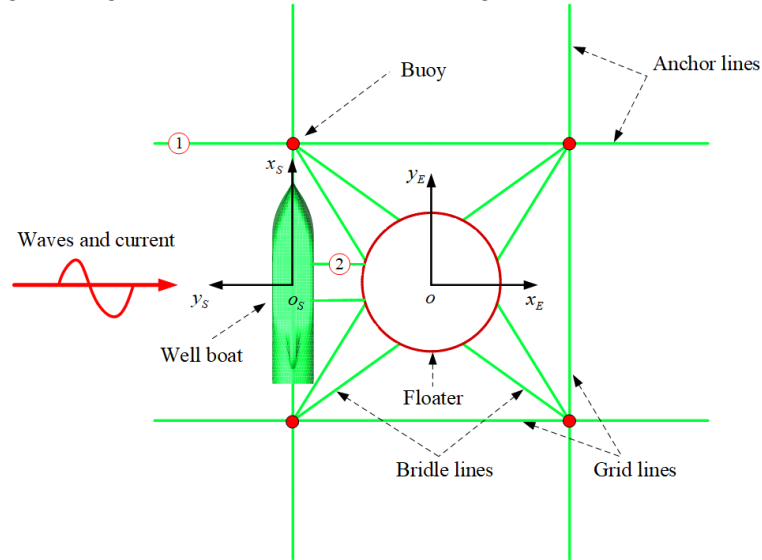

Figure 7. Configuration of the well boat and the moored fish-farm system with definitions of coordinate systems and wave and current directions.

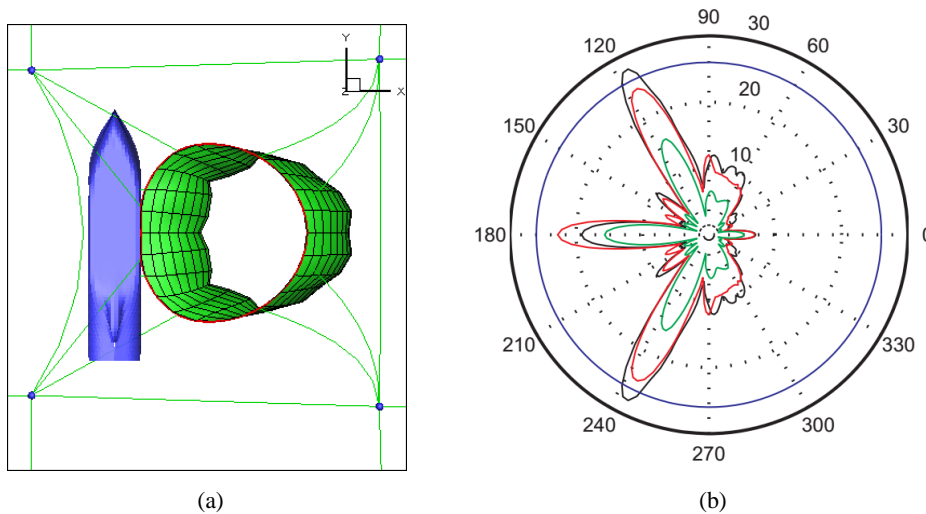(a)   (b)

Figure 8. (a) Well boat at a fish farm in regular waves and current. (b) Stress distribution along the floater due to horizontal deformations for cases with current velocity 0.6m/s and wave period T= 3s (green line), T=6s (red line) and T=9s (black line). The wave height-to-wave length ratio is 1/60. Blue line represents the yield stress (high-density polyethylene) (Shen et al. 2016).

2.6 Influence of fish on the mooring loads

He et al. (2017) studied experimentally the influence of fish in a net cage on mooring loads. Model tests in scale 1:25 were performed with more than 800 salmon of length 16cm inside a net cage in waves and current. The salmon occupied approximately 2.5% of the net cage volume at rest, which is representative for a full-scale condition. If the fish touched the netting, there was more than 10% increase in the mooring loads. The latter occurred in current only. Numerical calculations were made by changing the solidity ratio in the contact area between the fish and the net in such way that the numerical net configuration agreed with the experimental one. Good agreement between numerical and experimental values were obtained consequently. If the fish did not touch the netting, the loading influence was the order of 3%. An important question is if the fish behavior is representative for a full-scale scenario. If the fish do not touch the netting, an estimate of the net

10

loading can be made as follows. The fact that the fish displaces the water causes a flow and can be analyzed for a single fish by slender-body potential-flow theory; a first-order approximation of the far-field behavior can be obtained by summing up the individual contribution from each fish in terms of source distributions without considering the hydrodynamic interaction between the fishes. The latter procedure enables together with local ambient flow and realistic fish speeds to assess the importance of corresponding net loading by using the previously described net loading method. However, there are in addition a viscous wake due to the fishes and a flow caused by fish propulsion, which need to be quantified. The waves could cause the fish to go to the bottom of the net cage resulting in a non-negligible experimentally documented increase in mooring loads.

3 Wave and current load effects on closed floating fish farms

Closed fish cages can be divided into flexible cages (e.g. fabric) (see Figure 9), semi-flexible cages (e.g. GRP) and rigid cages (e.g. concrete or steel). They have typically a vertical symmetry axis at rest. A pump system is needed for water exchange in the tank and waste must be removed from the tank. The water inside a closed cage causes statically destabilizing roll and pitch moments. The shape and tension of a flexible cage in calm water depends on the density differences of water inside and outside the cage as well as overfilling of the cage. If current is present, the static shape and tension in the membrane is influenced by the current. The drag coefficient for closed fish farms in current has a very different behavior than shown for a net cage in Figure 3. Since the vertical flow velocity can be approximated as zero on the mean free surface, the presence of the free surface has an influence. When flow separation occurs from curved surfaces, there is influence of turbulent or laminar boundary layer flow on separation lines. Full scale conditions are typically in the supercritical flow regime and surface roughness can matter. When flow separation occurs from curved surfaces, scaling of model tests requires attention. When considering theoretically the effect of current, we must rely on CFD to describe the separated flow and account for hydroelasticity for the flexible closed cages.

Wave-induced sloshing (interior wave motion) becomes an issue as well-known from many engineering applications (Faltinsen and Timokha, 2009). Since marine applications involve relatively large excitation amplitudes, resonant sloshing can involve important nonlinear free-surface effects. The viscous boundary layer damping is very small. However, if breaking waves occur, the associated hydrodynamic damping is not negligible.

Lateral tank excitations with periods near the highest natural sloshing period are of primary concern. The highest natural sloshing period in rigid half-filled spherical tank of radius R_0 is $T_{11} = 2\pi\sqrt{R_0 / 1.56016g}$ with g as acceleration of gravity. The highest natural period $T_{1,1}$ as a function of the radius R_0 for an upright rigid circular cylindrical tank for different liquid depths h is presented in Figure 10. Structural elastic membrane effects for flexible cages (Strand and Faltinsen, 2017) will influence the natural sloshing frequencies.

Experimental and theoretical studies of sloshing in a vertical circular cylinder with horizontal harmonic forcing show that different overlapping wave regime involving planar waves, swirling waves and irregular chaotic waves occur (see Figure11) (Faltinsen and Timokha, 2009). Irregular chaotic waves mean that no steady-state condition occur while the planar and swirling waves are steady state. The waves are a consequence of nonlinear transfer of energy between sloshing modes. Which wave regime occurs depends on initial and transient conditions. Swirling waves have been of particular concern in designing spherical LNG tanks. A reason is the large horizontal forces occurring with components in-line and perpendicular to the forcing direction. It matters for the tank support and in the buckling analysis of the sphere.
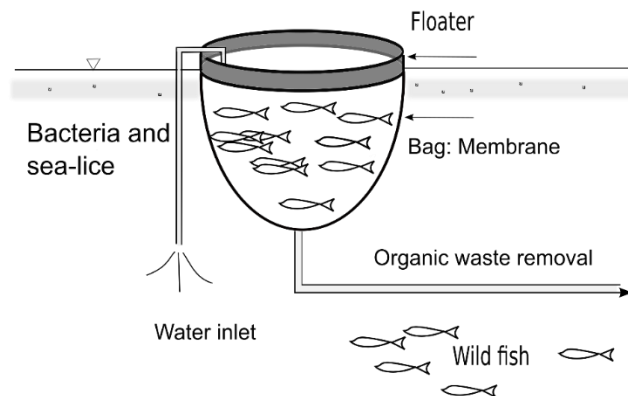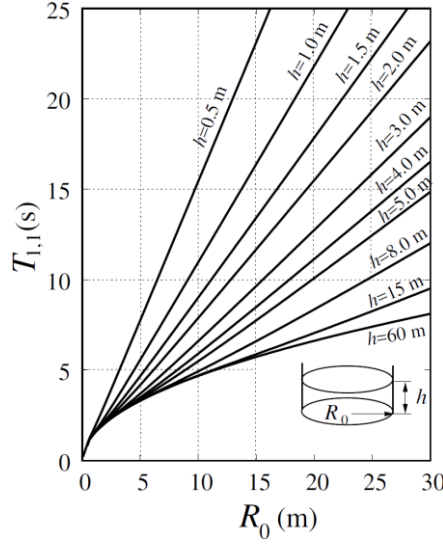
Figure 10. The highest natural period $T_{1,1}$ as a function of the radius R_0 for an upright rigid circular cylindrical tank for different liquid depths h (Faltinsen and Timokha, 2009).
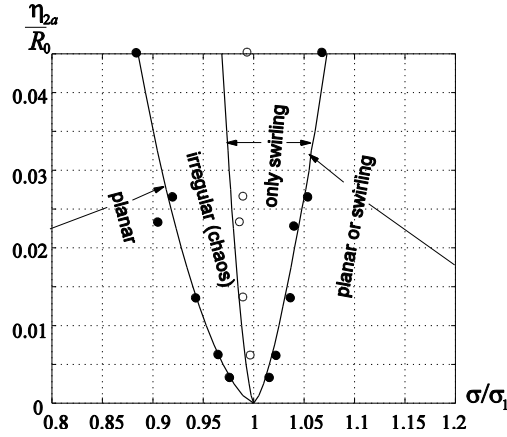

Figure 11. Effective frequency domains for stable steady-state waves and chaos in the $(\sigma / \sigma_1, \eta_{2a} / R_0)$-plane for an upright circular cylindrical tank with $h / R_0 = 1.5$. η_{2a} is forcing amplitude in sway. σ is forcing frequency. σ_1 is the first natural sloshing frequency. The bounds between the domains are obtained by using the multimodal theory (solid lines). Experimentally predicted bounds are taken from Royon-Lebeaud et al. (2007): ● = bounds for planar waves, ○ = bound for swirling (Faltinsen and Timokha, 2009).

There is important coupling between sloshing and the external flow through the body motions. When considering flexible cages, we must account for normal and tangential deformations of the membrane structure. In the 2D analysis by Strand (2018), the motion of the membrane is represented as the sum of rigid body motions and Fourier series with zero displacement at the attachment to the floater. Strong coupling between elastic modes and rigid body motions occurs. The finite static curvature of the membrane provides coupling between the normal and tangential deformations. The fact that the tangential deformations depend on the elastic properties of the membrane matters in model tests. It is insufficient with Froude scaling and geometric similarity. Proper scaling of model tests requires that Froude number and $Ed / \rho g L^2$ are the same in model and prototype scales. Here E, d, ρ, g and L are Young's modulus of elasticity, membrane thickness, water density, acceleration of gravity and a characteristic cage length, respectively. It is difficult with common length ratios in model and prototype scales to find materials with proper values of Ed in model scales. Structural damping is an unknown parameter. Dynamic and static membrane tension can become of the same magnitude in relatively small sea states and bending stiffness may have to be considered. Since the total tension cannot be negative, the

consequence can be snap loads. Strand (2018) has analyzed the problem in 2D without ambient current by using linear frequency-domain potential flow theory of incompressible water both for the interior and external flows. The interior flow problem is analyzed in a tank-fixed coordinate system moving with the rigid-body motions. The free-surface conditions differ in the exterior and interior flow problems. Extensive verifications were done. For instance, conservation of energy for the external flow problem relates uncoupled radiation wave damping for the flexible mode to far-field wave amplitudes. Furthermore, generalization of the Newman (1962) relations relate generalized excitation force of different normal modes to wave radiation damping of these modes. The wave-induced behavior is very different from rigid body cases and it is important in the future to perform experiments to validate the method. Very large inside free-surface elevations are predicted at the first and third natural sloshing frequencies in the considered frequency range, which implies that free-surface nonlinearities must be considered.

While nonlinearities must be considered for sloshing, the exterior potential flow can in some cases be based on linear time-domain boundary conditions within potential flow theory of incompressible water. Exceptions are when flow separation occurs and when considering wave drift forces. Flow separation occurs always with sharp corner When there are no sharp corners, flow separation in combined current and waves depends on the Keulegan- Carpenter number and the ratio between the current velocity and the incident wave-velocity amplitude (Faltinsen, 1990). Wave drift forces are needed in a mooring analysis, which can be based on a second-order analysis for the exterior flow problem. The coupled effect of sloshing has to be accounted for, which cannot be described as a weakly nonlinear system in resonant sloshing conditions. Current can have a non-negligible effect on wave drift forces. Since potential-flow wave drift forces are related to waves generated by the structure, care is needed in model tests to minimize tank-wall interference. Dependent on what the natural periods are in surge and sway, nonlinear slowly varying loads may also have to be considered as it is done for moored floating offshore structures with spread mooring systems.

If sloshing occurs in non-shallow water condition and there are no breaking waves, the nonlinear multimodal method (Faltinsen and Timokha, 2009) can describe the global sloshing loads in a time-efficient way. The multimodal method represents the free-surface elevation in terms of a Fourier-type series and the velocity potential as a sum of the product of generalized coordinates and the linear eigenmodes of sloshing. The boundary value problem is transferred by the Bateman-Luke formulation to a system of nonlinear ordinary differential equation for the generalized

coordinates of the free surface elevation. An advantage of the multimodal method is that acceleration dependent loads are explicit, which stabilizes the numerical time integration. Rognebakke and Faltinsen (2003) used the multimodal method and coupled the internal and external flows in 2D studies with finite water internal tank depth. It shows for pure sway motions and linear sloshing theory that zero response occur at a natural sloshing frequency. The reason is infinite added mass associated with the interior flow. Since the added mass associated with sloshing is frequency dependent, resonances in the sway motion occur. The numerical studies by Rognebakke and Faltinsen (2003) showed that nonlinear free-surface effects mattered in describing the sloshing part. The numerical results were validated by experiments.

Since violent sloshing implies nonlinear transfer of energy from the lowest sloshing mode, we can avoid exciting the lowest sloshing mode by properly moving a tank wall in an elastic manner (Faltinsen and Timokha, 2009). It requires a control system where the body motions are monitored. Another possibility to be further explored is to use air turbines to extract the sloshing wave energy. One could also introduce compartments to prevent swirling and to lower the highest natural sloshing period to a range where operational and extreme wave conditions do not cause significant resonant sloshing. It is difficult by flow separation from baffles to cause sufficient damping of sloshing.

4 Conclusions

The paper is partly a review on hydrodynamic and structural aspects of fish farms. In addition, new numerical results are presented on the stochastic behavior of bending stresses in the floater of a realistic net cage in extreme wave conditions. The behavior of traditional type fish farms with net cages and closed fish farms in waves and current are discussed. Hydroelasticity plays a significant role for net cages and closed membrane-type fish farms. The many meshes in a net cage make CFD and complete structural modeling impracticable. As an example, a hydrodynamic screen model and structural truss elements are instead used to represent the hydrodynamic loading and the structural deformation of the net. In addition, the wake inside the net due to current plays an important role. The described simplified numerical method has been validated by comparing with model tests of mooring loads on a single net cage with two circular elastic floaters and bottom weight ring in waves and current. It is discussed which parts of the complete system play the most important roles in accurately determining the mooring loads. Important uncertainties are description of the wake inside a net and how much of the current flow that goes through the net. Many realizations of a sea state

13

are needed to obtain reliable estimates of extreme values in a stochastic sea. The latter fact is commonly neglected in model tests. Many net cages operate in close vicinity, which raises questions about spatial variations of the current and wave environment as well as hydrodynamic interaction between the net cages. Wave interaction becomes of importance for closed fish farms.

It has been shown by model tests that live fish touching the netting can have a non-negligible influence on the mooring loads. An uncertainty is if the fish behave differently in full-scale conditions.

Important future studies are snap loads in netting, bridle lines and vertical support chain/rope between floater and sinker tube. Snap loads should also be of concern for membrane-type closed fish farms. Uncertainty analysis of prediction methods for mooring loads on fish farms should be further pursued.

It is demonstrated by numerical calculations in waves and current that a well boat at a net cage can have a significant influence on mooring loads and bending stresses in the floater. The latter results provide a rational way to obtain operational limits for a well boat at a fish farm. However, the approach and departure phases of a well boat need also to be studied. Maneuvering in waves becomes then an issue.

Sloshing matters in describing the behavior of a closed fish farm when important wave frequencies are near natural sloshing frequencies. The structural flexibility has to be accounted for in determining the natural sloshing frequencies for a membrane-type closed fish farm. Free-surface nonlinearities can matter for sloshing and can, for instance, result in swirling in a certain frequency domain for a closed cage with a vertical symmetry axis. There is a need to develop numerical methods that can describe nonlinear sloshing in a closed fish farm in a time efficient way to predict probability density functions of relevant response variables in operational and survival sea states. The multimodal method for sloshing is a candidate. Mean and slowly varying drift forces must be considered in a mooring analysis for a closed fish farm.

Model tests of membrane-type closed fish farms require that the elastic properties are properly scaled. The latter seems in practice to be impossible.

Acknowledgements

References

Bardestani, M., Faltinsen, O. M. 2013. A two-dimensional approximation of a floating fish farm in waves and current with the effect of snap loads, *Proc. 32nd International Conference on Ocean, Offshore and Arctic Engineering*, pp.V009T12A020-V009T12A020. June 9-14, Nantes, France.

Dong, G. H., Xu T. J., Zhao Y. P., Li Y. C., et al. 2010. Numerical simulation of hydrodynamic behavior of gravity cage in irregular waves. *Aquacultural Engineering*. 42(2), 90-101.

Faltinsen, O. M. 1990. *Sea Loads on Ships and Offshore Structures*. Cambridge University Press, Cambridge, 228-238.

Faltinsen, O. M., Timokha, A. N. 2009. *Sloshing*. Cambridge University Press, Cambridge, 135.

[FAO] Food and Agriculture Organization. 2006. The State of World Aquaculture. FAO Fisheries technical paper 500, Rome. 134 pp.

Field, C. B., Behrenfeld, M. J., Randerson, J. T., Falkowski, P. 1998. Primary Production of the Biosphere: Integrating Terrestrial and Oceanic Components. *Science*. 281(5374), 237-240.

He, Z., Faltinsen, O. M., Fredheim, A., Kristiansen, T. 2017. The influence of fish on the mooring loads of a floating net cage. *Journal of Fluids and Structures*, **76**, 384-395.

Huang, C. C., Tang, H. J. and Liu, J. Y. 2006. Dynamical analysis of net cage structures for marine aquaculture: Numerical simulation and model testing. *Aquacultural Engineering*, 35(3), 258-270.

Huang, C. C., Tang, H. J. and Liu, J. Y. 2008. Effects of waves and currents on gravity-type cages in the open sea. *Aquacultural Engineering*, 38(2), 105-116.

Kristiansen, T., Faltinsen, O. M. 2012. Modeling of current loads on aquaculture net cages, *Journal of Fluids and Structures*, 34, 218-235.

Kristiansen, D., Faltinsen, O. M., 2009, Nonlinear wave induced motions of cylindrical-shaped floaters of fish farms, *Proc. Inst. Mech. Eng, Part M, Journal of Engineering for the Marine Environment*, 223(3), 361-375.

Kristiansen, T., Faltinsen, O. M., 2014, Experimental and numerical study of an aquaculture net cage with floater in waves and current, *Journal of Fluids and Structures*, 54, 1-26.

Le Bris, F., Marichal, D., 1998. Numerical and experimental study of submerged supple nets applications to fish farms. *Journal of Marine Science Technology* 3, 161–170.

Li, P., Faltinsen, O. M. 2012. Wave-induced vertical response of an elastic circular collar of a floating fish farm, *Proc. Tenth International Conference on Hydrodynamics (ICHD 2012)*, October 1-4, St. Petersburg, Russia. 2, 58-64.

Li P., Faltinsen O.M., Greco, M. 2018. Wave-induced accelerations of a fish-farm elastic floater: experimental and numerical studies, *J. of Offshore Mechanics and Arctic Engineering*, 140(1), pp. 011201.

Li, P, Faltinsen, O. M., Lugni, C. 2016. Nonlinear vertical accelerations of a floating torus in regular waves, *Journal of Fluids and Structures,* 66, 589-608.

Løland, G. 1991. *Current Forces on and Flow through Fish Farms*. Dr. Ing. thesis. Division of Marine Hydrodynamics. The Norwegian Institute of Technology.

Marichal, D., 2003. Cod-end numerical study. In: Third International Conference on Hydroelasticity in Marine Technology, Oxford, UK. 3, 11-18.

Naess, A., Moan, T. 2012. *Stochastic Dynamics of Marine Structures*. Cambridge University Press, Cambridge University Press, New York, 176-179.

Rognebakke, O. F., Faltinsen, O. M. 2003. Coupling of sloshing and ship motions, *J. Ship Res.,* **47**, 3, 208-221.

NAS, 2009. NS 9415 Marine fish farms-Requirements for site survey, risk analysis, design, dimensioning, production, installation and operation. ICS 65. 150;67.260. Standards Norway. Norway. (http://www.standard.no), 21-22.

Newman, J. N., 1962. The exciting forces on fixed bodies in waves, *J. Ship Res.,* **6**, 4, 10-17

Royon-Lebeaud, A., Hopfinger, W. J., Cartellier, A., 2007. Liquid sloshing and wave breaking in circular and square-base cylindrical containers. *J. Fluid Mech. 577*, 467-494.

Shainee, M., Leira, B. J., Ellingsen, H and Fredheim, A. 2014. Investigation of a self-submersible SPM cage system in random waves. *Aquacultural Engineering.* 58, 35-44.

Shen, Y. G., Greco, M., Faltinsen, O. M. 2016. Numerical study of a coupled well boat-fish farm system in waves and current during loading operations, *12th International Conference on Hydrodynamics, ICHD2016*, Egmond aan Zee, The Netherlands. Online proceedings, document No.98.

Shen, Y. G., Greco, M., Faltinsen, O. M., Nygaard, I. 2018. Numerical and experimental investigations on mooring loads of a marine fish farm in waves and current. *Journal of Fluids and Structures*.79, 115-136.

Strand, I. M., Faltinsen, O. M. 2017. Linear sloshing in a 2D rectangular tank with a flexible sidewall. *Journal of Fluids and Structures*. 73, 70-81.

Strand, I. M. 2018. *Sea Loads on Closed Flexible Fish Cages.* PhD thesis. Department of Marine Technology. Norwegian University of Science and Technology, Trondheim, 37-40.

Xu, T. J., Dong, G. H., Zhao, Y. P., Li, Y. C., et al. 2011. Analysis of hydrodynamic behaviors of gravity net cage in irregular waves. *Ocean Engineering*. 38(13), 1545-1554.

Xu, T. J., Zhao, Y. P., Dong, G. H and Gui, F. K. 2013. Analysis of hydrodynamic behavior of a submersible net cage and mooring system in waves and current. *Applied Ocean Research*. 42, 155-167.

Xu, T. J., Zhao, Y. P., Dong, G. H., Li, Y. C., et al. 2013. Analysis of hydrodynamic behaviors of multiple net cages in combined wave-current flow. *Journal of Fluids and Structures.* 39, 222-236.